



Low temperature oxidation of CO using alkali- and alkaline-earth metal-modified ceria-supported metal catalysts: a review

JYOTI WAIKAR and PAVAN MORE* 

Department of Chemistry, Institute of Chemical Technology, Mumbai 400019, India

*Author for correspondence (pm.more@ictmumbai.edu.in)

MS received 11 March 2021; accepted 12 July 2021

Abstract. The present review devoted to the complete oxidation of CO using alkali- and alkaline-earth metal (AM/AEM)-modified ceria supported/mixed with noble metal and non-noble metal (NM). The AM/AEM-modified Ce supported/mixed with noble metal showed comparable CO oxidation with unmodified catalyst. However, AM/AEM-modified NM showed higher CO oxidation at lower temperature compared to the unmodified catalyst. The AM and AEM modifications were responsible for the formation of oxygen vacancies in Ce, which leads to the decrease in the CO and O₂ activation barrier. The dissociative oxygen adsorption on AM/AEM-modified Ce-supported/mixed with NM favours the CO oxidation at a lower temperature. However, AM/AEM-modified Ce-supported/mixed with noble metal showed CO adsorption with formation of superoxy and peroxy species, which leads to the comparable oxidation activity. The plausible mechanism for CO oxidation is explained in detail with correlation to the characterizations.

Keywords. CO oxidation; CeO₂ modification; noble metal; non-noble metal; alkali metal; alkaline-earth metal.

1. Introduction

The expeditious growing society and rapid industrialization are responsible for the number of pollutants released into the atmosphere. Major pollutants include greenhouse gases, organic and inorganic compounds, volatile organic compounds and carbon monoxide (CO). These pollutants contribute in the adverse variations of the atmosphere and are mainly due to the incomplete combustion of fossil fuel. The major primary source of pollutants is vehicle transport and industrial exhaust [1,2]. CO is the most toxic gas released into the atmosphere by incomplete combustion of carbonaceous materials [3]. Hence, major efforts have been taken to inhibit the emission of pollutants. There are variety of methods reported for emission control of CO, such as adsorption, absorption, thermal combustion, condensation, catalytic oxidation, etc. Among them, catalytic oxidation is the simple and affordable method for CO oxidation [4–6]. Researchers have used various noble metal and non-noble metal (NM) catalysts for CO oxidation. Noble metals like Au, Pd, Pt and Rh show good activity for CO oxidation [7–11]. In spite of having the good catalytic activity of noble metal catalysts, their practical and environmental applications are restricted due to limited sources, high price and poisoning [12]. However, various mixed oxide catalysts like hydroxalicates, spinel oxides, perovskites, transition metal oxides and supported NM catalysts, etc. have been used for CO oxidation [13–19]. Furthermore, the three-way catalytic

converter (TWC) operated at higher temperature (>297°C) restricts the oxidation of CO and other pollutants throughout the cold start time. Therefore, the preparation of cost-effective and low temperature oxidation catalyst is the recent target in the automotive industry [20]. Ceria with metal/metal oxide could be an alternative to overcome these drawbacks. Ceria-supported catalyst are used with noble metals like Pt and Pd, which show the higher activity for CO oxidation. The Ce showed facile redox properties and oxygen storage capacity (OSC). Therefore, Ce showed superior catalytic performance compared to the other metal oxides [21–24]. OSC of Ce assures the constituents of gases during air/fuel back and forth motion by releasing and storing oxygen under fuel-lean and rich conditions, respectively [25]. Maximum OSC of Ce was responsible for maintaining the availability of oxygen during fuel-lean and rich conditions. However, Ce alone is not effective for CO oxidation. Therefore, modification of Ce could be done by adding noble metal and/or NM. The formation of nanorod of ceria due to the interaction with NM increases the low temperature CO oxidation [26]. The modification can be done by changing the lattice structure and deposition of metal. The loading of metals on the Ce surface provides the active sites between metal and Ce interface for CO oxidation. Therefore, the combination of metal with Ce is a promising approach towards low temperature activity. Furthermore, alkali metal (AM) and alkaline-earth metal (AEM) could serve as a textural and electronic promotor for

catalysts in various processes. Hence, many researchers have tried to improve low temperature activity in recent years through modification of support by AMs and AEMs [27–30].

The activity of metal-supported on Ce catalyst is controlled by particle size, interaction between metal and support, morphology and OSC. Thus, it is obligatory to develop a systematic perspective to improve low temperature CO oxidation. Alkali acts as an electron promotor to enhance the surface redox properties and is responsible for the low temperature CO and VOC oxidation [31–34]. The CO oxidation activity of noble metal and NM supported on ceria was enhanced by addition of AM and AEM [35–38]. AM and AEM showed different solubility in ceria lattice. The larger metal ion shows the least solubility compared to the smaller AM and AEM [39]. The maximum solubility of smaller AM and AEM leads to the improvement in the surface porosity and electronic properties of ceria lattice. The variation in solubility of these metal/metal oxides increased the OSC of ceria. The OSC was responsible for release and storage of the oxygen in modified ceria catalyst, which enable the low temperature CO oxidation. In this study, the effect of AM- and AEM-modified CeO₂ support responsible for low temperature activity has been reviewed in detail. The improvement in low temperature CO oxidation activity of metal-supported ceria due to the AM and AEM has been highlighted here with plausible mechanism.

2. CO oxidation using modified CeO₂

The ceria is used for reduction and oxidation reactions due to the unique properties. The oxygen vacancies in Ce improves the oxygen dispersion rate in lattice and was responsible for higher catalytic activity [40]. These vacancies were observed due to the parameters like temperature, nature of dopant, oxygen pressure, and electrical field controlled during synthesis [41]. Ceria showed OSC due to reversible transformation within Ce³⁺ and Ce⁴⁺ and provide the oxygen during oxygen-deficient condition. Furthermore, the reduction of CeO₂ to CeO_{2-δ} (2-δ = O/Ce) leads to the formation of defect occurrence (oxygen vacancy) as a Ce³⁺ ion. The lattice oxygen desorbs from CeO₂ surface and oxygen leaves two electrons on Ce⁴⁺ cation. These two electrons filled the empty 4f orbital of Ce⁴⁺ to generate Ce³⁺. Hence, Ce³⁺ can be a potent indicator for oxygen vacancy formation [42]. The CeO₂ surface oxygen vacancy (V_o) having lattice plane (111) is thermodynamically stable in cubic structure and having active surface lattice plane (111) [43,44]. The literature reveals that the crystal planes are strongly influenced by morphology of the material, which affects the reactivity of the catalyst [45–47]. Piumetti *et al* [48] theoretically reported the oxygen vacancies formation energy order of Ce for various planes (110) < (100) < (111). Sayle *et al* [49] demonstrated that the (100) and (110) surface planes were

catalytically and thermodynamically active for CO oxidation compared to (111) surface planes. Therefore, the Ce with (100) and (110) planes showed higher activity than (111) plane due to the movement of lattice oxygen from bulk to surface of catalyst.

The incorporation of other elements into ceria lattice is an important approach towards increase in V_o formation and low temperature CO oxidation activity. The substitution of other elements of lower valency could be responsible for the formation of defects and lattice distortions due to the presence of V_o. Ce⁴⁺ has ionic radius 0.97 Å compared to the dopant (lower or higher ionic radius), which affects the energy of V_o formation. Nolan [50] examined the V_o formation in ceria after doping with Al, Sc, In, Y and La having ionic radii 0.39, 0.75, 0.80, 0.96 and 1.16 Å, respectively. He found that the doped element with radii close to Ce easily fit within the lattice. However, smaller and larger ionic radii strongly distort the structure, which leads to the increase in V_o formation required for maximum CO oxidation. Further, Gupta *et al* [51] reported density functional theory study of ceria doped with transition metals like Mn, Fe, Co, Ni, Cu, Pd, Pt, Ru, rare-earth metals, etc., and showed improvement in redox properties and OSC. Whereas, rare-earth metals showed negligible increment in OSC. Transition metal and noble metal ions showed very strong structural distortion by forming long and short cation-oxygen bonds, favourable for CO oxidation activity.

Furthermore, Liu *et al* [52] observed the maximum CO oxidation activity of Cu_x-CeO₂ catalyst due to strong interaction between CuO_x and CeO₂. The optimum amount of Cu doping on CeO₂ and its calcination temperature showed significant effect on catalytic performance than pure CeO₂. The CO oxidation activity of Cu_x-CeO₂ is shown in figure 1. Cu/Ce (molar ratio 0.09) calcined at 600°C showed maximum CO oxidation at 110°C than pure CeO₂ (280°C). The maximum well-dispersed Cu⁺ species was responsible for the oxidation of CO at a lower

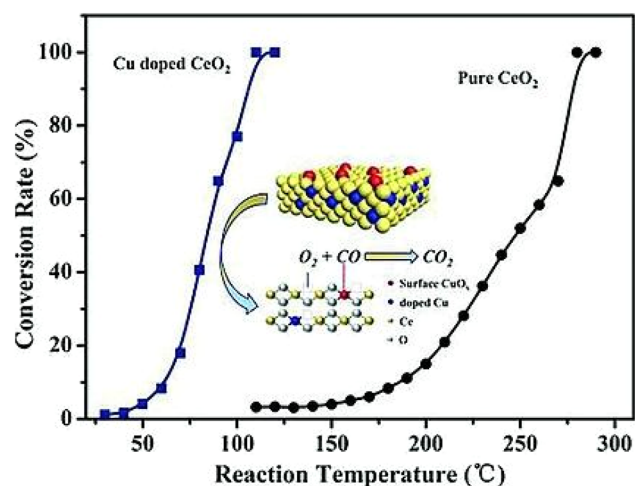
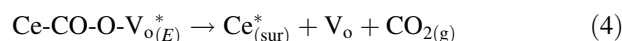
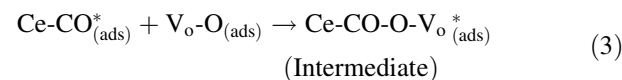


Figure 1. CO oxidation activity on pure CeO₂ and Cu-doped CeO₂. Reproduced with the permission from [52].

temperature. The V_o facilitates the formation of maximum Cu^+ species on the catalyst surface.

The low temperature activity of CeO_2 could be increased by addition of the active metal. The metal mixed with/supported on CeO_2 showed three plausible reaction mechanisms related to catalytic CO oxidation, like Langmuir Hinshelwood (LH), Eley-Rideal (ER) and Mars-van Krevelen (MvK). Among three mechanisms, in MvK the catalyst surface is an active reaction component and is used to describe the consecutive CO oxidation [53–58]. However, Ce is well known for defective structure and oxygen vacancies. Therefore, CO oxidation on ceria is explained by MvK mechanism. In MvK mechanism, the catalyst surface is an active reaction integrant responsible for CO oxidation [59]. The different sources of oxygen for oxidation have been reported. However, one of them is lattice oxygen of Ce and another is from gaseous oxygen activated by V_o [57,60]. The conventional and carbonate-mediated MvK CO oxidation mechanism is shown in figure 2. The mechanism includes CO_2 formation and its desorption, leaving an oxygen vacancy. This is an endothermic reaction and depends on the mobility of lattice oxygen towards the surface. The energy required to remove lattice oxygen corresponds to energy of oxygen vacancy formation and correlated with the CO oxidation activity of doped and undoped CeO_2 . However, the energy is vital for low temperature CO activity and depends on the nature of doping metal. Typically, according to MvK mechanism (equations 1–4) CO adsorb on the CeO_2 active site (Ce^*) and gaseous oxygen adsorbed on oxygen vacancies (V_o). The adsorbed CO and surface oxygen (O_{surf}) could react and form an

intermediate ($Ce-CO-O-V_o^*_{(ads)}$). The intermediate further forms $CO_{2(g)}$ with the regeneration of active sites. The CO also reacts with lattice oxygen (O_L) to form CO_2 and regeneration of oxygen vacancy (V_o) takes place. The active site could be regenerated by adsorption of gas-phase O_2 .



Furthermore, Liu *et al* [61] reported the carbonate-mediated mechanism on Co-doped Ce (110) surface. The mechanism is shown in figure 2. The formation of carbonate as an intermediate on various metal-doped CeO_2 surfaces was described in detail. CO adsorbed on the Co and interact with lattice oxygen to form carbonate intermediate. This intermediate further interacts with adsorbed CO to form two linear CO_2 molecules with two oxygen vacancies and carbonate as an intermediate. The nature and coordination of dopant metal is responsible for low temperature CO conversion through MvK mechanism. In conventional mechanism, Co-doped Ce containing (111) and (100) surface showed adsorption of CO on lattice oxygen and forms linear CO_2 intermediate, which easily desorbed from the surface. In this type of mechanism, only one oxygen vacancy was regenerated.

Moreover, the modification of CeO_2 by the addition of meta/metal oxide has been reported to improve the

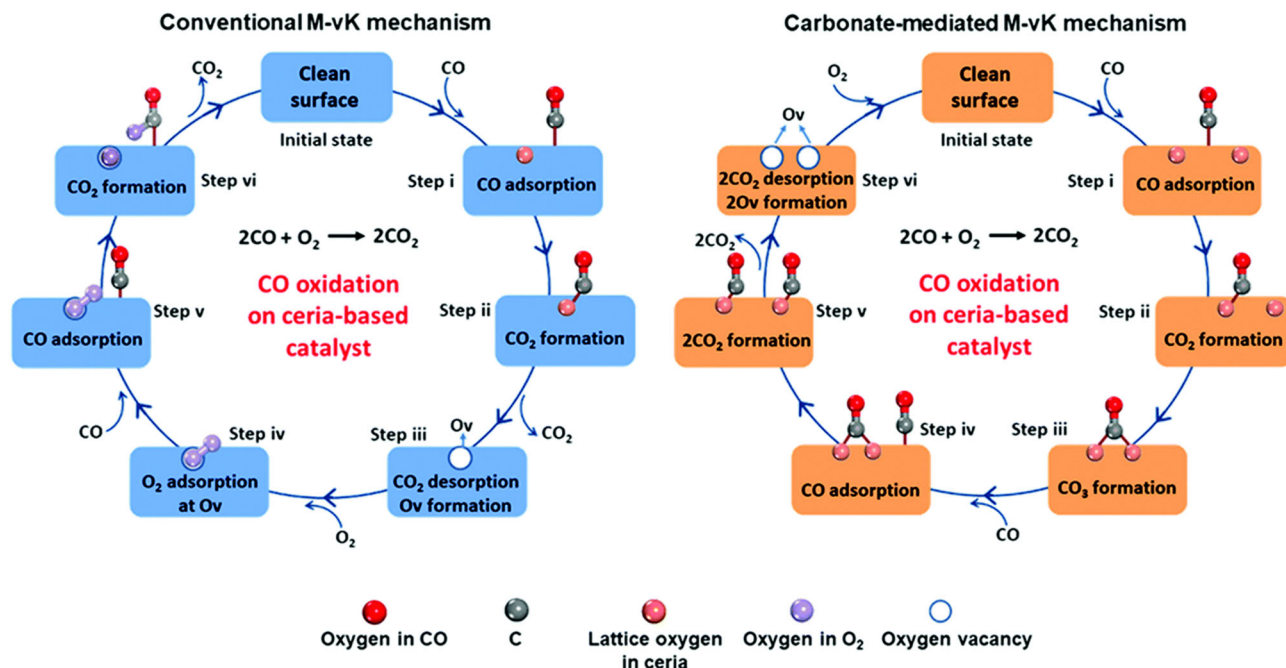


Figure 2. Conventional carbonate-mediated MvK mechanism on co-modified CeO_2 for CO oxidation to CO_2 . Reproduced with the permission from [61].

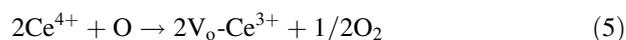
physicochemical properties required for low temperature CO oxidation [62]. Zou *et al* [63] studied the adsorption phenomenon on Ce catalyst doped with AM and AEM. The CuO-CeO₂ is reported for preferential oxidation of CO in H₂-rich conditions. The carbonyl species desorption was observed at lower temperature. However, at higher temperature formation of carbonate species was observed over CuO-CeO₂. The doping of AM/AEM (Li/Ba) in CuO-CeO₂ showed irreversible adsorption of CO, which inhibits the adsorption of H₂. The AM/AEM also favours the formation of format by maximum CO adsorption compared to the CuO-CeO₂. Moreover, researchers are taking the efforts to improve the low temperature oxidation activity through modification of CeO₂ by doping with precious metals, transition metals, lanthanides, AE, AEM, etc. The noble metal and NM supported/mixed with CeO₂ modified by the addition of AM and or AEM. The modification of Ce catalyst by AEM and AM could lead to the improvement in redox properties. The ionic radii of AM and AEM showed comparable variation than Ce, which could lead to the generation of lattice distortion in the crystal and forms active sites for oxidation.

2.1 Effect of AM and AEM doping on noble metal (M) mixed with/supported on CeO₂ on CO oxidation

The noble metal supported on/mixed with ceria has been studied widely for oxidation of VOC and CO. However, low temperature activity of these catalysts could be improved by the addition of third metal. Gluhoi and Nieuwenhuys [64] prepared the BaO (AEM)-modified Au supported on Al₂O₃ and CeO₂, and studied for CO oxidation at room temperature. AEM oxides stabilize small Au particles against sintering. Guo *et al* [65] studied series of AEMs like Mg, Ca, Sr and Ba-modified Pd/CeO₂ catalysts. The AEM-doped CeO₂ enhances the number of defects in the crystal lattice and oxygen vacancies, which was responsible for the high oxidation activity. Anguita *et al* [66] studied the effect of biofuel impurities like AM, AEM and phosphorus on CO, NO and propene oxidation activity of PtPd/CeZr/La-Al₂O₃. The lower electronegativity of AM (Na = K < Ca) and higher metal oxygen interaction lead to enhancement in the reduction temperature. However, the broadness of peaks increases after the addition of AM and could be due to the electron donating ability of AM. Therefore, AM could be responsible for the increase in adsorption of CO on the catalyst surface, which leads to the saturation and requires higher temperature for desorption of CO and O₂ as a CO₂. The support of PtPd/CeZr/La-Al₂O₃ modified Na, K, Ca and P. The P-modified PtPd/CeZr/La-Al₂O₃ showed lower light-off temperature. However, catalyst showed comparable activity with Na-, K-, Ca-modified PtPd/CeZr/La-Al₂O₃ (PtPd) catalyst above 200°C. The H₂-TPR analysis is shown in figure 3. The temperature programmed reduction (TPR) profiles showed shifting of

H₂-TPR peaks towards higher temperatures. The H₂-TPR peaks temperature order are PtPd < aged-PtPd < P-PtPd < Ca-PtPd < K-PtPd < Na-PtPd. The electron donating ability of the AM increases reduction of temperature towards the higher side.

Furthermore, table 1 shows the comparison of CO oxidation of AM- and AEM-modified noble metal mixed/supported on CeO₂. AM- and AEM-modified oxides are considered as structural promoters for CO oxidation due to the strong interaction with noble metals and CeO₂. The AEM-modified catalyst showed higher CO conversion (T₁₀₀) at lower temperature compared to the AM-modified catalyst. The doping of aliovalent metals in CeO₂ leads to the formation of V_o on the CeO₂ surface. The reduction of CeO₂ to CeO_{2-δ} was observed and represented by Kroger-Vink equation (5) [67].



In reduced conditions, doubly charged oxygen vacancy (V_o) and Ce³⁺ are formed in the lattice of ceria. These V_o generates two electrons, which further accepted by two Ce⁴⁺ ions and reduced to Ce³⁺ with the formation of oxygen vacancies. The plausible MvK mechanism for the oxidation of CO by AM- and AEM-doped noble metal supported/mixed with CeO₂ is shown in equations 6–15. The formation of active oxygen species (O* = O²⁻, O⁻, O₂⁻) was observed due to the adsorption of gaseous oxygen on V_o as shown in equations 6 and 7. AM and AEM have the ability to donate the electrons and therefore enhance the mobility of active oxygen species. These species were regenerated by gaseous oxygen (equation 9). The CO adsorbed on the CeO₂, noble metal and AM/AEM interface. The CO adsorption leads to the reduction of Ce⁴⁺ to Ce³⁺ (equation 8). The active oxygen species (O* = O²⁻, O⁻, O₂⁻) is formed by transfer of electron from AM/AEM to Ce⁴⁺

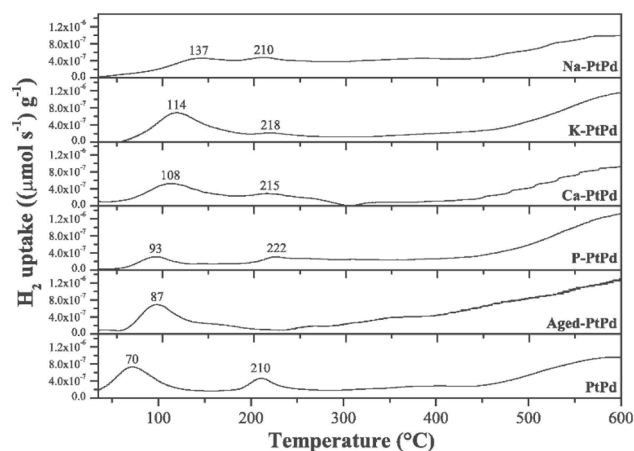


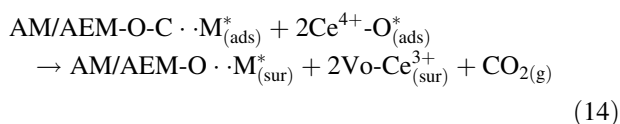
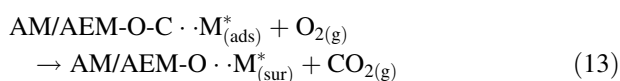
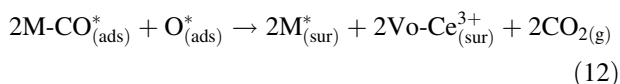
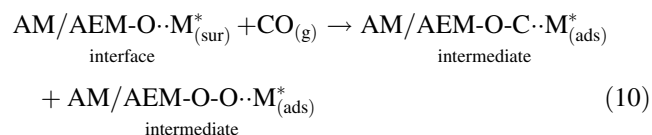
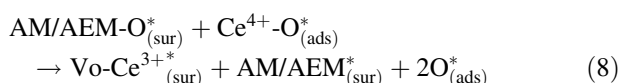
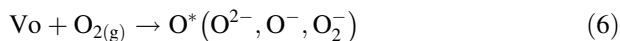
Figure 3. H₂-temperature programmed reduction profile of fresh, aged and modified catalysts (conditions: 2% H₂ in Ar flow with 50 ml min⁻¹, temperature 25–650°C with rate 2°C min⁻¹). Reproduced with the permission from [66].

Table 1. Comparison of CO oxidation activity of AM- and AEM-doped noble metal-modified CeO₂.

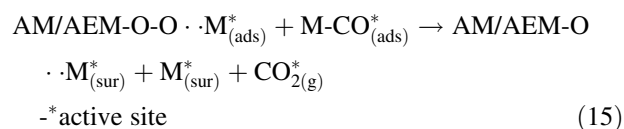
Catalyst	T ₁₀₀ (°C)	Reaction condition	References
Na-PtPd	200	300 ppm CO, 10% O ₂ , with He balance, H ₂ O 3.5% GHSV = 135000 h ⁻¹	[57]
K-PtPd	200		
Ca-PtPd	190		
Pt-Pd	180		
Au/CeO _x /Al ₂ O ₃	120		
Au/BaO/CeO _x /Al ₂ O ₃	RT	CO and O ₂ (4% He balance), GHSV = 2500 h ⁻¹ , CO/O ₂ = 2/1	[60]
Au/Li ₂ O/CeO _x /Al ₂ O ₃	100		
Au/Rb ₂ O/CeO _x /Al ₂ O ₃	152		

species (equation 8). However, gaseous oxygen interacts with oxygen vacancy and leads to the formation of active oxygen species (O^{*}). The noble metals (M) could be a good active site for CO adsorption than gaseous oxygen [59]. Moreover, CO adsorbed on metal further reacts with active oxygen. The desorption of CO₂ takes place with the regeneration of oxygen vacancies and active metal species (equations 11 and 12). The dissociative adsorption of CO [68] takes place on noble metal and AM/AEM interface, which could form the intermediates (equation 10). These intermediates could react with CO adsorbed on metal, gaseous oxygen and or oxygen adsorbed on V_o (equations 12–15).

Furthermore, the AM/AEM-doped noble metals showed desorption of CO₂ at higher temperature [69] compared to the undoped noble metal mixed/supported on Ce. The AM/AEM doping showed negative effect on the oxidation activity due to the adsorption of CO₂ on the surface, which blocks the active sites.

**Table 2.** Light off, T_{50%} and T_{100%} CO conversion temperature of Mg-modified MnCe (0.5:0.5 mol) and Mg- and Cs-modified CuCe (0.15:0.185 mol) [72–74].

Catalyst	Temperature (°C)		
	Light-off	T ₅₀	T ₁₀₀
0.125 wt% MgMnCe	35	104	157
6 wt% MgCuCe	40	56	100
CuCe	40	70	100
MnCe	77	119	163
1 wt% Pt/Al ₂ O ₃	147	195	209
0.1 wt% CsCuCe	40	60	100



2.2 Effect of AM and AEM doping on NM supported on/mixed with CeO₂ on CO oxidation

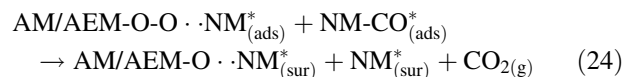
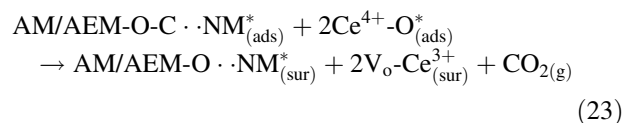
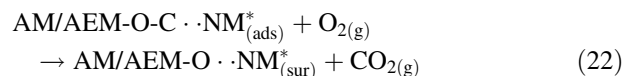
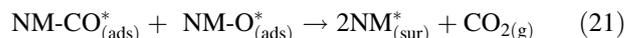
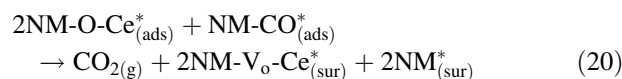
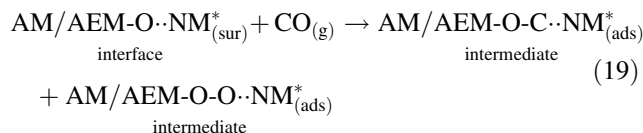
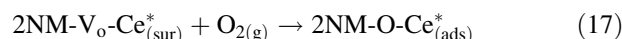
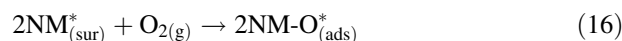
The AM (Cs) is electronic or textural promoters for NM mixed/supported on ceria catalyst used for oxidation reactions. In an oxidation reaction, electron-donating effect of AM enhances the reactivity of oxygen in metal–oxygen bond. Similarly, AEMs like Mg, Sr, etc. act as a promotor for NM mixed/supported on ceria for methane reforming, Fischer tropsch synthesis, VOC oxidation, NO_x reduction, soot oxidation and water-gas shift reaction, etc. [70,71]. The comparison of light-off temperature, 50% (T₅₀) and 100% (T₁₀₀) CO conversion temperature of Mg-doped MnCe, CuCe and Cs-doped CuCe is shown in table 2. In our previous study, Mg-modified MnCe and Cs and/or Mg-modified CuCe catalyst reported for CO oxidation separately [72,73]. Lavande *et al* [72,74] prepared Mg-doped Mn and Cu-modified CeO₂ (MnCe and CuCe) for complete CO oxidation. The concentration of Mg doping on MnCe and CuCe has been optimized for CO oxidation. The 0.125 and 6 wt% Mg-doped MnCe and CuCe, respectively, showed higher CO oxidation at lower temperature. Similarly, the concentration of Cs doping on CuCe optimized for CO

oxidation. However, 0.125 wt% Mg-doped MnCe catalyst showed higher CO oxidation at light-off temperature compared to the 6 wt% MgCuCe. Whereas, 50 and 100% CO conversion of 6 wt% MgCuCe was observed at lower temperature compared to the 0.125 wt% Mg-doped MnCe, 0.1 wt% CsCuCe, CuCe, MnCe and commercial inhouse prepared 1 wt% Pt/Al₂O₃. The order of 50% CO conversions (T_{50}) are 6 wt% MgCuCe < 0.1 wt% CsCuCe < CuCe < 0.125 wt% MgMnCe < MnCe < 1 wt% Pt/Al₂O₃. The increase in low temperature CO conversion was observed on Cs- and Mg-modified CuCe compared to remaining of the catalyst. The Mg and Cs doping in CuCe lead to the generation of defects in the lattice and consequently form the active oxygen species responsible for low temperature activity. Mg and Cs show synergistic interaction with Ce, which is responsible for the active oxygen vacancies and increases the dispersion of metal on catalyst surface.

Furthermore, Fan *et al* [75] prepared the Sr-modified CeO₂ and ZrO₂ by coprecipitation and impregnation method and correlated the OSC of catalyst with CO oxidation. The OSC measurement was carried out by CO pulse method and the order is Sr/CeO₂/ZrO₂ (impregnation method) > Sr/CeO₂/ZrO₂ (coprecipitation method) > CeO₂/ZrO₂. The Sr/CeO₂/ZrO₂ catalyst prepared by the impregnation method showed higher OSC than the undoped CeO₂/ZrO₂ and Sr/CeO₂/ZrO₂ prepared by the coprecipitation method. The Sr was acting as a structural promoter and enhances the reducibility of a catalyst with the formation of SrZrO₃ phase. The SrZrO₃/CeO₂-ZrO₂ interface and high OSC was responsible for higher CO oxidation activity. Furthermore, An *et al* [76] reported the OSC of Ca- and Mg-doped CeO₂/ZrO₂. The CeO₂/ZrO₂ catalyst doped with Mg showed higher OSC compared to Ca-doped catalyst. However, OSC results of these Mg- and Ce-doped CeO₂/ZrO₂ are compared with OSC of Sr-doped CeO₂/ZrO₂. The order of OSC is ($\mu\text{mol CO}_2 \cdot \text{g}_{\text{cat}}^{-1}$) CeZrMgO₂ > CeZrCaO₂ > Sr/CeO₂/ZrO₂ (impregnation method) > Sr/CeO₂/ZrO₂ (coprecipitation method) > CeO₂/ZrO₂.

The increase in OSC due to Ca was attributed to the proper ionic radius of Ca and maximum solubility of Ca in Ce-Zr lattice compared to the Mg. The higher OSC indicates the increase in oxygen mobility from bulk to surface and the formation of oxygen vacancies. Moreover, Ce⁴⁺ reduced to Ce³⁺ due to the doping with AEM. The improvement in OSC was responsible for the increase in CO oxidation activity. Furthermore, the plausible mechanism of CO oxidation using AM/AEM-modified NM mixed/supported on Ce is shown in equations (16–24). The oxygen and CO adsorption takes place on V_o and NM, respectively. The AM and AEM doping enhances the formation of V_o due to electron donating capacity and was responsible for the CO activation at lower temperature. AM/AEM interacts readily with oxygen to form active oxygen species and acts as oxygen donor for the oxidation reaction. NMs like transition metals as well as the metals having unpaired electrons are used as a catalyst due to

their variable oxidation states. NMs redox behaviour and synergistic interaction with Ce^{4+/3+} redox couple are responsible for the formation of O* species equations (6 and 7) and leads to the higher oxidation activity. The interaction of AM/AEM and NM with CeO₂ forms V_o in the vicinity of Ce³⁺ equation (8), which leads to the formation of active NM-O* and NM-O-Ce* species equations (16 and 17). Unlike noble metal, NM activates the gaseous oxygen and forms active NM-O* equation (16). Furthermore, NM reacts with CO to give NM*-CO_(ads) equation (18). AM/AEM and NM interface could activate CO at lower temperature than NM-supported ceria equation (19). AM/AEM have the ability to donate electrons to the active species, which enhance the reducibility of NM, and is a key factor for the desorption of adsorbed oxygen and improved the oxidation ability [77]. Furthermore, all these adsorbed species reacts and form CO₂ equations (20–24). Moreover, AM and AEM doping increases the CO adsorption on catalyst surface.



The activation of O₂ takes place on ceria and NM. The presence of AM/AEM lower the activation energy for noble metal and NM. However, O₂ and CO preferentially activated on the NM, whereas noble metal requires high energy for activation of O₂ and predominantly showed the CO adsorption than O₂. NM redox behaviour and synergistic interaction with Ce redox couple are responsible for the formation of active species and consequently enhance the oxidation activity. The *density functional theory* study shows that the O₂ activation takes place on noble metal through formation of peroxy and superoxy species, whereas NM showed dissociative adsorption of O₂. The primary step in the O₂ activation is adsorption. The remarkable amount of charge transfer takes

place from metal to the O₂ for strong chemisorption. However, O₂ adsorbed weakly on the NMs. Hence, O₂ dissociates with a low energy barrier. Metal with a low O₂ dissociation barrier could provide the atomic oxygen easily to the neighbouring species [78]. The formation of atomic oxygen on metal surface showed higher CO oxidation [79]. The NM predominantly showed formation of atomic oxygen species through dissociation. AM/AEM-modified NM mixed or supported on ceria showed decreases in activation energy required for dissociative adsorption of O₂, CO, formation of oxygen vacancies and OSC, which was responsible for the maximum CO oxidation at lower temperature. Therefore, enhancement in CO oxidation was observed in AM/AEM-modified NM catalyst compared to the noble metal catalyst.

3. Conclusion

The review summarizes the recent progress in the investigation of catalytic oxidation by AM- and AEM-modified noble and non-noble mixed/supported on CeO₂ catalyst. The fundamental mechanism of the low temperature CO oxidation showed the formation of various intermediates, which facilitate the CO oxidation. The modification by AM/AEM generates the defects in Ce lattice, which enhances the oxygen vacancies on the surface and also increases the OSC. These modification increases the mobility of active oxygen species from bulk to the surface of catalyst. Although CeO₂ is used in catalytic converter due to its unique properties, further research is necessary to understand the AM/AEM effect on its textural and structural properties, like Ce structure, OSC, oxygen vacancies and redox cycle Ce^{4+/3+}, to make it suitable and cost effective for various applications.

Acknowledgements

The WOS-A (Woman Scientist – A) grant from the Department of Science and Technology (KIRAN DIVISION) having project SR/WOS-A/CS-110/2018(G) and early career research award (ECR/2016/000823) from SERB-DST are acknowledged for financial support.

References

- [1] Katsouyanni K 2003 *Br. Med. Bull.* **68** 143
- [2] Montero-Montoya R, López-Vargas R and Arellano-Aguilar O 2018 *Ann. Glob. Heal.* **84** 225
- [3] Heck R M and Farrauto R J 2001 *Appl. Catal. A Gen.* **221** 443
- [4] Margitfalvi J L, Borbáth I, Hegedus M, Tfirst E, Gobolos S and Lazar K 2000 *J. Catal.* **196** 200
- [5] Rynkowski J and Dobrosz-Gómez I 2010 *Ann. UMCS Chem.* **64** 1

- [6] Rossignol C, Arrii S, Morfin F, Piccolo L, Caps V and Rousset J L 2005 *J. Catal.* **230** 476
- [7] Janssens T V W, Carlsson A, Puig-Molina A and Clausen B S 2006 *J. Catal.* **240** 108
- [8] Qin H, Qian X, Meng T, Lin Y and Ma Z 2015 *Catalysts* **5** 606
- [9] Ligthart D A J M, Van Santen R A and Hensen E J M 2011 *Angew. Chem.-Int. Ed.* **50** 5306
- [10] Liu H H, Wang Y, Jia A P, Wang S Y, Luo M F and Lu J Q 2014 *Appl. Surf. Sci.* **314** 725
- [11] Schubert M M, Plzak V, Garche J and Behm R J 2001 *Catal. Lett.* **76** 143
- [12] Deutschmann O, Knözinger H, Kochloeff K and Turek T 2011 *Ullmann's Encycl. Ind. Chem.* https://doi.org/10.1002/14356007.o05_o02
- [13] Royer S and Duprez D 2011 *ChemCatChem.* **3** 24
- [14] Ramesh K, Chen L, Chen F, Liu Y, Wang Z and Han Y F 2008 *Catal. Today* **131** 477
- [15] Liang S, Teng F, Bulgan G, Zong R and Zhu Y 2008 *J. Phys. Chem. C* **112** 5307
- [16] Shelef M and McCabe R W 2000 *Catal. Today* **62** 35
- [17] Wan H, Li D, Dai Y, Hu Y, Zhang Y, Liu L *et al* 2009 *Appl. Catal. A Gen.* **360** 26
- [18] Wang X, Huang K, Yuan L, Xi S, Yan W, Geng Z *et al* 2018 *J. Phys. Chem. Lett.* **9** 4146
- [19] Sie M C, Jeng P Di, Chen P H, Wu R C and Wang Bin C 2017 *AIP Conf. Proc.* **1877** 07004
- [20] Di Monte R and Kašpar J 2004 *Top Catal.* **28** 47
- [21] Carlsson P A and Skoglundh M 2011 *Appl. Catal. B Environ.* **101** 669
- [22] Reddy B M, Bharali P, Saikia P, Park S E, Van Den Berg M W E, Muhler M *et al* 2008 *J. Phys. Chem. C* **112** 11729
- [23] Li P, Chen X, Li Y and Schwank J W 2019 *Catal. Today* **90** 115
- [24] Kim H J, Jang M G, Shin D and Han J W 2020 *Chem. Cat. Chem.* **12** 11
- [25] Kašpar J and Fornasiero P 2003 *J. Solid State Chem.* **171** 19
- [26] Hossain S T, Azeeva E, Zhang K, Zell E T, Bernard D T, Balaz S and Wang R 2018 *Appl. Surf. Sci.* **455** 132
- [27] Tibiletti D, De Graaf E A B, The S P, Rothenberg G, Far-russeng D and Mirodatos C 2004 *J. Catal.* **225** 489
- [28] Xue L, He H, Liu C, Zhang C and Zhang B 2009 *Environ. Sci. Technol.* **43** 890
- [29] Shen Y F, Suib S L and O'Young C L 1994 *J. Am. Chem. Soc.* **116** 11020
- [30] Santos V P, Pereira M F R, Órfão J J M and Figueiredo J L 2009 *Appl. Catal. B Environ.* **88** 550
- [31] Ruiz M L, Lick I D, Ponzi M I, Rodriguez-Castellón E, Jiménez-López A and Ponzi E N 2011 *Appl. Catal. A Gen.* **392** 45
- [32] More R K, Lavande N R and More P M 2020 *Bull. Mater. Sci.* **43** 1
- [33] More R K, Lavande N R and More P M 2019 *Mol. Catal.* **47** 4110414
- [34] More R K, Lavande N R and More P M 2018 *Catal. Commun.* **116** 52
- [35] Qiao B, Wang A, Yang X, Allard L F, Jiang Z, Cui Y *et al* 2011 *Nat. Chem.* **3** 634
- [36] Shen W, Dong X, Zhu Y, Chen H and Shi J 2005 *Micropor. Mesopor. Mater.* **85** 157

- [37] Mock S A, Sharp S E, Stoner T R, Radetic M J, Zell E T and Wang R 2016 *J. Colloid Interface Sci.* **466** 261
- [38] Song S, Wang K, Yan L, Brouzgou A, Zhang Y, Wang Y et al 2015 *Appl. Catal. B Environ.* **176** 233
- [39] Pashalidis I and Theocharis C 2000 *Stud. Surf. Sci. Catal.* **128** 643
- [40] Lappalainen J, Tuller H L and Lantto V 2004 *J. Electrochem. Soc.* **151** 129
- [41] Herman G S 1999 *Surf. Sci.* **437** 207
- [42] Alaydrus M, Sakaue M and Kasai H 2016 *Phys. Chem. Chem. Phys.* **18** 12938
- [43] Alessandro T 2002 *Catalysis by ceria and related materials (World Scientific)* vol 2 p 528
- [44] Wu L, Wiesmann H J, Moodenbaugh A R, Klie R F, Zhu Y, Welch D O et al 2004 *Phys. Rev. B-Condens. Matter Mater. Phys.* **69** 1
- [45] Si R and Flytzani-Stephanopoulos M 2008 *Angew. Chem.-Int. Ed.* **47** 2884
- [46] Mai H X, Sun L D, Zhang Y W, Si R, Feng W, Zhang H P, Liu H C et al 2005 *J. Phys. Chem. B* **109** 24380
- [47] Ta N, Liu J and Shen W 2013 *Chin. J. Catal.* **34** 838
- [48] Piumetti M, Bensaid S, Russo N and Fino D 2015 *Appl. Catal. B Environ.* **165** 742
- [49] Sayle T X T, Parker S C and Sayle D C 2005 *Phys. Chem. Chem. Phys.* **7** 2936
- [50] Nolan M 2011 *J. Phys. Chem. C* **115** 6671
- [51] Gupta A, Waghmare U V and Hegde M S 2010 *Chem. Mater.* **22** 5184
- [52] Liu B, Li Y, Cao Y, Wang L, Qing S, Wang K and Jia D 2019 *Eur. J. Inorg. Chem.* **2019** 1714
- [53] Spezzati G, Benavidez A D, DeLaRiva A T, Su Y, Hofmann J P, Asahina S et al 2019 *Appl. Catal. B Environ.* **243** 36
- [54] Qin L, Cui Y, Deng T, Wei F and Zhang X 2018 *Chem. Phys. Chem.* **2** 3346
- [55] Kim H Y and Henkelman G 2013 **2** 2
- [56] Vandichel M and Grönbeck H 2018 *Top. Catal.* **16** 1458
- [57] Puiggollers A R, Schlexer P, Tosoni S and Pacchioni G 2017 *ACS Catal.* **7** 6493
- [58] Kim Hyung Jun, Jang Myeong Gon, Shin Dongjae and Han Jeong Woo 2020 *Nanotech.* **8** 11
- [59] Waikar J, Pawar H and More P 2019 *Chem. Eng.* **2** 11
- [60] Fadzil N A M, Rahim M H A B and Pragas Maniam G 2018 *Mater. Res. Express.* **5** 085019
- [61] Liu B, Li W, Song W and Liu J 2018 *Phys. Chem. Chem. Phys.* **20** 16045
- [62] Venkataswamy P, Jampaiah D, Mukherjee D, Aniz C U and Reddy B M 2016 *Catal. Lett.* **146** 2105
- [63] Zou H, Chen S, Liu Z and Lin W 2010 *Powder Technol.* **30** 672
- [64] Gluhoi A C and Nieuwenhuys B E 2007 *Catal. Today* **122** 226
- [65] Guo T, Nie X, Du J and Li J 2018 *RSC Adv.* **8** 38641
- [66] Anguita P, García-Vargas J M, Gaillard F 2018 *Chem. Eng. J.* **352** 333
- [67] Nolan M, Fearon M, Watson J E and Graeme W 2006 *Solid State Ion.* **177** 3069
- [68] Rodriguez J A, David G C, Ramírez P J, Stacchiola D J and Senanayake S 2018 *J. Phys. Chem. C* **122** 4324
- [69] Yu Q, Chen W, Li Y, Jin M and Suo Z 2010 *Catal. Today* **158** 324
- [70] Rico-Pérez V, Aneggi E and Trovarelli 2017 *Catalysts* **7** 28
- [71] Shi C and Zhang P 2015 *Appl. Catal. B Environ.* **170** 43
- [72] Lavande N R, More R K and More P M 2020 *Appl. Surf. Sci.* **502** 144299
- [73] Waikar J M, More R K, Lavande N R and More P M 2021 *J. Rare Earths* **39** 434
- [74] Waikar J M, Lavande N R, More R K and More P M 2020 *Asia* **24** 269
- [75] Fan J, Weng D, Wu X, Wu X and Ran R 2008 *J. Catal.* **258** 177
- [76] An Y, Shen M and Wang J 2007 *J. Alloys Compd.* **441** 305
- [77] Aneggi E, de Leitenburg C, Dolcetti G and Trovarelli A 2008 *Catal. Today* **136** 3
- [78] Motemore M, Spronsen M A, Madix R J and Friend C M 2018 *Chem. Rev.* **118** 2816
- [79] Widmann D and Behm R J 2014 *Acc. Chem. Res.* **47** 740